Microbial controls over soil priming effects under chronic nitrogen and phosphorus additions in subtropical forests

Jian Li[1,2,3], Zhan-Feng Liu[1*], Ming-Kang Jin[2,3], Wei Zhang[1], Hans Lambers[4,5], Dafeng Hui[6], Chao Liang[7], Jing Zhang[1], Donghai Wu[1], Jordi Sardans[8,9], Josep Peñuelas[8,9], Dan Petticord[10], David W. Frey[10], Yong-Guan Zhu[2,3,11*]

[1]*Key Laboratory of Vegetation Restoration and Management of Degraded Ecosystems & CAS Engineering Laboratory for Vegetation Ecosystem Restoration on Islands and Coastal Zones, South China Botanical Garden, Chinese Academy of Sciences, Guangzhou, China*

[2]*Key Laboratory of Urban Environment and Health, Ningbo Observation and Research Station, Institute of Urban Environment, Chinese Academy of Sciences, 1799 Jimei Road, Xiamen 361021, China*

[3]*Zhejiang Key Laboratory of Urban Environmental Processes and Pollution Control, C.A.S. Haixi Industrial Technology Innovation Center in Beilun, Ningbo 315830, China*

[4]*School of Biological Sciences, University of Western Australia, Perth, Western Australia, Australia*

[5]*Department of Plant Nutrition, College of Resources and Environmental Sciences; National Academy of Agriculture Green Development; Key Laboratory of Plan-Soil Interactions, Ministry of Education, China Agricultural University, Beijing, China*

[6]*Department of Biological Sciences, Tennessee State University, Nashville, Tennessee, USA*

[7]*Institute of Applied Ecology, Chinese Academy of Sciences, Shenyang 110016, China*

[8]*CSIC, Global Ecology Unit, CREAF-CSIC-UAB, Bellaterra, 08193 Barcelona, Catalonia, Spain*

[9]*CREAF, Cerdanyola del Vallès, 08193 Barcelona, Catalonia, Spain*

[10]*Department of Ecology & Evolutionary Biology, Cornell University, Ithaca, NY, 14850, USA*

[11]*State Key Laboratory of Urban and Regional Ecology, Research Center for Eco-Environmental Sciences, Chinese Academy of Sciences, Beijing 100085, China*

***Authors for correspondence:**

Yong-Guan Zhu

Address: Key Laboratory of Urban Environment and Health, Ningbo Observation and Research Station, Institute of Urban Environment, Chinese Academy of Sciences, 1799 Jimei Road, Xiamen 361021, China.

E-mail: ygzhu@rcees.ac.cn

Zhan-Feng Liu

Address: Key Laboratory of Vegetation Restoration and Management of Degraded Ecosystems, South China Botanical Garden, Chinese Academy of Sciences, Guangzhou 510650, China.

E-mail: liuzf@scbg.ac.cn

Type of article: Research article

R**unning title:** Microbial controls over soil priming effects

Number of figures and tables: 2 tables and 4 figures

Supporting information: 2 tables and 11 figures

Main body of text: 4833 words

Abstract

The soil priming effect, where labile carbon inputs affect soil organic matter decomposition, is known to influence carbon (C) storage in terrestrial ecosystems. Priming, however, is a product of several complex microbial interactions and the extent to which chronic nutrient addition, such as that brought on by the Anthropocene, may influence soil priming is unknown. Further, plant physiology, such as differences in microbial community between leguminous and non-leguminous rhizosphere, will affect PE through interaction with nutrient (e.g., nitrogen) access capacity, is still unclear. Therefore, we collected soils from beneath leguminous and non-leguminous subtropical plantation areas across a suite of historical nutrient addition regimes. We added ^{13}C-labeled glucose to investigate how background soil nutrient conditions and microbial community affect priming and its potential microbial mechanisms. Glucose addition increased soil organic matter decomposition and prompted positive priming in all soils, regardless of dominant overstory tree species or fertilizer treatment. In non-leguminous soil, only combined nitrogen and phosphorus addition led to a higher positive priming than the control. Conversely, soils beneath N-fixing leguminous plants responded positively to P supplementation alone, as well as to the joint NP addition when compared to control. Using DNA stable-isotope probing and high-throughput quantitative PCR, we found that positive priming effects were associated with increased microbial C utilization, accompanying an improvement of microbial community activity, nutrient-related gene abundance, and enzyme activities. Our findings suggest that the regulation of nutrient availability

on the priming effect is influenced by the balance between soil available N and P, depending on rhizosphere microbial community composition. Furthermore, these findings highlight the roles of the interaction between plant physiology and microbial community in regulating soil priming and improve our understanding of the potential microbial pathway underlying soil priming effects.

Keywords: Carbon utilization, DNA-SIP, Enzyme activity, Functional genes, Nutrient addition, Microbial community, SOM decomposition

Introduction

Soil organic matter (SOM) is the largest terrestrial carbon pool, and therefore, a slight change in SOM decomposition rates can greatly impact atmospheric CO_2 concentrations and global climate[1, 2]. The decomposition of SOM is mainly driven by soil microorganisms, and this process is strongly affected by exogenous labile carbon (C) inputs [3, 4]. A sufficient increase in the amount of labile carbon can "jumpstart" decomposition, much like priming a pump. This positive feedback, where an increase in labile carbon can increase the rate of SOM decomposition, is consequently referred to as "positive priming effects" [5, 6]. On a global scale, the priming effect can increase the decomposition rate of SOM by up to 60% and enhance the release of CO_2 from the soil by up to 50% [7, 8]. Given rising concerns about atmospheric carbon levels, and an increased global prioritization for the conservation of soil carbon sinks, it is essential to understand better the priming effect on soil C cycling, better to improve our measurement and estimation of soil C dynamics [9, 10].

Although research on priming effects has been increasing rapidly in recent years, it can be challenging to pin down an exact mechanism. Priming can vary in magnitude and direction among systems, which makes it challenging to predict [4, 11, 12]. This substantial variation can be attributed to many factors, such as differences in microbial community composition and their functional traits[12–15]. Soil microorganisms, as the main decomposers of SOM, play an understandably huge role

in SOM priming [4, 16]. The complexity of belowground microbial interactions makes predicting the influence of the soil microbiome difficult, but not impossible. For example, research suggests that the variation of microbial biomass and the ratio between r and K-strategists within microbial communities can strongly affect the priming effect [11, 16, 17]. The increased availability of high-throughput sequencing data has allowed us to identify important taxa that may control decomposition. For instance, recent work demonstrates that specific microbial taxa, such as *Proteobacteria* and *Acidobacteria* can contribute to SOM decomposition, and they may play a crucial role in regulating the soil priming effect [18, 19]. In addition, breakthroughs in microbial functional gene suggest that these microbial nutrient-related cycling genes (e.g., genes related to C, N, and P decomposition and acquisition) is closely linked to SOM decomposition and might be the key to understand the priming effect [20–23]. These interactions between soil microbiome, microbial gene expression and priming effect remain complex, however, demanding further investigation. Moreover, variations in microbial biomass, function, and composition can impact SOM priming, and therefore, factors that impact microbial communities, such as soil nutrient availability, can also affect priming.[3, 12, 24]. For instance, variation in available soil nitrogen (N) can have extensive effects on soil microbial biomass, activity, composition, and enzyme activity, all which ultimately affect SOM decomposition [25, 26]. Microbial decomposition is often linked to Sprengel-Liebig's Law of the Minimum (growth is dictated not by total resources available, but by the scarcest resource) or stoichiometric decomposition theory

(Microbial activity is highest and decomposition rates are greatest if the inputs of C and N match the microbial demand for substrate, i.e., the inputs corresponds to stoichiometric C and N ratios) [11, 27, 28], wherein microbial decomposition ability should be constrained by the scarcest nutrient. This principle is further complicated by global patterns of nutrient deposition, which have greatly influenced ecosystem nutrient balances, particularly in the tropics. For example, an increase in available P may not be accompanied by an increase in N, altering the stoichiometry between bioavailable N and P [25, 29].

Tropical and subtropical forest ecosystems account for a large part of the total global forest area and soil organic C stocks [30, 31]. These highly weathered ecosystems are often P-limited, and any P latent to the system is often bound to oxides and hydroxides of aluminum and iron, given the highly acidic soil and high levels of cation bridging [29, 32]. In addition, tropical and subtropical forests have been increasingly regarded as N deposition hotspots with potentially harmful influences on forest health and biodiversity due to the increased rapid consumption of N fertilizers and fossil fuels in recent decades [33, 34]. Increasing rates of N deposition may further exacerbate this P deficiency as it likely disturbs a previously balanced rate of consumption between N and P in ecosystems [35, 36]. This increasing P limitation would suggest that P addition would dramatically improve growth in these systems, improving their carbon storage capacity. In addition, soil priming is also impacted by

plant physiology, and species-specific microbial communities around plant roots may lead to species-level variation in priming responses [37, 38]. This physiological difference may extend to broad plant functional categories. Legumes, for example, can obtain additional N from the atmosphere through symbiotic N_2 fixation by rhizobia bacteria [39, 40]. In this case, soil priming may be less influenced by abiotic N than by abiotic P, as the N demands of the plant can be met through facultative mutualisms. Under the assumptions we laid out above, we would imagine a commensurately stronger influence of P in leguminous plants that are simultaneously capable of meeting an increased N demand through rhizomatous N-fixation. Therefore, we hypothesized that phosphorus addition has a greater effect on priming effects in legume soils. We further hypothesized that nutrient addition improves microbial carbon utilization by influencing the microbial community structure and their activities, such as the functional gene expression and enzyme activity, which in turn induces greater priming effects. To test these hypotheses, we collected soil from one plantation dominated by an N-fixing tree species (*Acacia auriculiformis*) and another dominated by a non-N-fixing tree species (*Eucalyptus urophylla*) exposed to 10 years of N and/or P addition. We then conducted a soil incubation experiment, where ^{13}C-labeled glucose was added as the labile C input, to understand how N and P availability impact SOM priming and its underlying microbial processes in soils growing different plant functional types.

Materials and methods

Study sites and field treatments

The study site was located at the Heshan National Field Research Station of Forest Ecosystems (112°50′E, 22°34′N) in southern China. The region has a tropical monsoon climate, with a mean annual precipitation of 1580 mm, 80% of which occurs from April to September. The annual temperature is approximately 22°C, ranging from 12.6°C (January) to 28.0°C (July) [41]. Study sites were located in two forest plantation types, dominated by either leguminous plants (LP) or non-leguminous plants (NLP). Both plantations sampled in this study are over 30 years old. The dominant species in the canopy layer of the LP plantation was *Acacia auriculiformis*. The predominant species of the NLP plantation was *Eucalyptus urophylla*. The soil in both plantations could be classified as acrisol (FAO, 2006) and soil properties were summarized in Table 1.

The N and P field addition experiment was established with a complete randomized block design in August 2010. The field experiment included a control plot without nutrient addition (henceforth CK), an N-addition treatment of 100 kg N ha^{-1} yr^{-1} (henceforth N)), a P-addition treatment of 100 kg P ha^{-1} yr^{-1} (henceforth P), and an N+P-addition treatment of 100 kg of both N and P ha^{-1} yr^{-1} (henceforth NP). Treatments were applied to 10 m x 10 m plots in three separate locations (blocks) in each plantation (Fig. S1). Ammonium nitrate (NH_4NO_3) and/or sodium biphosphate

183 (NaH_2PO_4) dissolved in 10 L of water was used for the additional treatments, and
184 these solutions were sprayed bimonthly. To keep water consistent between plots, the
185 CK plot received 10 L of water at the time of nutrient addition treatments.

186

187 Ten soil samples were randomly collected from the upper 20 cm soil layer of each
188 plot and mixed homogeneously into a single composite soil sample. In this fashion, a
189 total of 24 (4 nutrient treatments × 2 plantations × 3 replicates) soil samples were
190 collected. Soil samples were transported to the lab immediately and passed through a
191 2-mm sieve.

192

193 **Incubation experiment**

194 Soil samples were adjusted to 40% water-holding capacity and then pre-incubated in a
195 climate-controlled room (~22 °C) for one week before the start of the incubation
196 experiment to allow settling after the sampling and sieving disturbance [42, 43]. Pre-
197 incubated soil from each treatment was weighed and divided into eight equal parts of
198 40 g each and placed into 50 mL vials. Vials were then placed into 2 L headspace
199 chambers with lids. In total, 48 headspace chambers contained eight vials each (4
200 nutrient treatments × 2 plantations × 3 replicates × 2 parallels). The priming effect
201 was calculated by adding demineralized purified water containing dissolved ^{13}C-
202 glucose to the vials (hereafter referred to as glucose treatment). This resulted in a C

addition of ~450 µg C/g fresh soil, equivalent to the average microbial biomass C in all soil samples. Control vials received an equal amount of demineralized purified water (hereafter referred to as control). All headspace chambers were incubated in the dark in a climate-controlled room at ~22°C, matching the annual average temperature at the field site [41]. After incubation for 0, 6, 18, 42, 66, 114, and 162 hours, soil respiration and available N were measured. Soil C substrate utilization, microbial biomass, phospholipid fatty acids, and potential enzyme activities were measured at the end of the incubation (Fig. S2).

Soil respiration and priming effect

At each time point (0, 6, 18, 42, 66, 114, and 162 hours), one vial was removed from the headspace for analysis. After being removed from the headspace chamber, the vial was placed into a 1-L airtight bottle equipped with a catheter. The headspace was purged with CO_2-free air before the bottle was closed with a lid. The bottles were incubated for 5–24 hours at 22° C in the dark, depending on the time required to obtain enough CO_2 [42]. Then, the gas was collected into an airbag, and the CO_2 concentration and its isotopic composition ($^{13}C/^{12}C$ ratio) were measured using a Picarro G2201-i analyzer (Picarro Inc., Santa Clara, CA, USA). The released CO_2 that originated from SOM and glucose was calculated using the following equations:

$$f_{glucose} = (\text{atom\% } {}^{13}C_{CO2} - \text{atom\% } {}^{13}C_{SOM}) / (\text{atom\% } {}^{13}C_{glucose} + \text{atom\% } {}^{13}C_{SOM})$$

223 $f_{SOM} = 1 - f_{glucose}$

224 $R_{SOM} = R_{total} \times f_{SOM}$

225 $R_{glucose} = R_{total} - R_{SOM}$

226 Where $f_{glucose}$ and f_{SOM} are the fractions of released CO_2 derived from glucose and
227 SOM, respectively, and atom% $^{13}C_{glucose}$ and atom% $^{13}C_{SOM}$ represent the atom% ^{13}C
228 in glucose and SOM, respectively. The total released CO_2 (R_{total}) was then partitioned
229 into CO_2 released from SOM decomposition (R_{SOM}) and CO_2 released from the
230 breakdown of glucose ($R_{glucose}$).

231 The priming effect was then calculated as the difference in the released CO_2 from
232 SOM between samples with and without glucose addition:

233 Priming effect ($\mu g\ C\ g^{-1}$ soil) = $R_{SOM\ with\ glucose} - R_{SOM\ in\ control}$

234 Priming effect (%) = $(R_{SOM\ with\ glucose} - R_{SOM\ in\ control}) \times 100\% / R_{SOM\ in\ control}$

235 Where $R_{SOM\ with\ glucose}$ is the CO_2 released from SOM with glucose addition treatment,
236 $R_{SOM\ in\ control}$ is the CO_2 released from SOM in control without glucose addition.

237

238 **Soil properties and microbial biomass**

239 Before the incubation, soil pH was determined in a 1: 5 ratio of soil and water slurry
240 using a combination glass electrode meter (FiveEasyPlusTM FE28, Mettler Toledo,
241 Switzerland), as well as soil organic carbon (SOC), soil total N (TN), soil inorganic

nitrogen (IN), soil total P (TP), and soil available P (AP) concentrations were determined following protocols as described previously [44]. Microbial biomass C (MBC) and N (MBN) concentrations were determined by the chloroform fumigation method [45]. After the incubation, total microbial biomass was first determined by phospholipid fatty acid analysis (PLFA) using freeze-dried soil as previously [46], with minor modifications [13]. Then the microbial ^{13}C incorporated into biomass was calculated based on the atom% ^{13}C excess in bacterial and fungal biomarker PLFAs determined by the GC-C-IRMS system [3].

Microbial DNA extraction and ultracentrifugation

Soil microbial DNA was extracted from 0.5 g soil using NDA extraction kit (MP Biomedicals, Santa Ana, CA, USA) before and after the ^{13}C-glucose addition incubation experiment. This DNA was further purified using a MO BIO purification kit (Carlsbad, CA, USA).

Ultracentrifugation was used to separate the ^{13}C-DNA and ^{12}C-DNA since the ^{13}C-DNA is heavier than the ^{12}C-DNA. Briefly, 3.0 μg microbial DNA was dissolved in 1.85 g/mL CsCl with the density adjusted by adding buffer (0.1 M pH = 8.0 Tris-HCl, 0.1 M KCl, 1.0 mM EDTA) or CsCl. The prepared DNA solution was transferred to a Beckman ultra-high-speed centrifugal tube and centrifuged at 177,000 ×g at 20°C for

44 h by an NTV-100 vertical rotor (Beckman Coulter, Palo Alto, CA, USA). The DNA solution was fractionated to 13 layers using a fixed velocity pump (New Era Pump Systems, Inc., Farmingdale, NY, USA) after centrifugation. The refractive index of each DNA layer was measured using a refractometer (Reichert Inc., Buffalo, NY, USA), and the DNA buoyant density was calculated based on the refractive index. All separated layer DNA was purified using polyethylene glycol 6000 precipitation and then stored in a freezer at -20°C.

PCR amplification, DNA sequencing, and high-throughput quantitative PCR

Quantitative real-time polymerase chain reaction (qPCR) was used to quantify the DNA in each layer on a CFX96 Optical Real-Time Detection System (Bio-Rad, Laboratories Inc., Hercules, CA, USA) [47, 48]. The labeled DNA is expected to have a density of approximately 1.725 g/ml [48, 49], therefore, ultracentrifugal DNA fractions with a density between 1.69 and 1.75 g/ml were used for further sequencing and high-throughput quantitative PCR. Bacterial 16S rRNA was amplified with primers F515 and R907 [50], and primers ITS1F and ITS2R [51] were used for fungal ITS. Sequencing was performed in the Hiseq 2000 system at Shanghai Majorbio Bio-pharm Technology Co., Ltd. Raw sequence data were filtered using Trim Galore software, and paired sequences were spliced using the FLASH2 software. The taxonomy of amplicon sequence variants (ASVs) was analyzed by QIIME2 against

the 16S rRNA database (Silva v138), we followed a DADA2 pipeline to denoise the optimized sequences after quality control.

High-throughput qPCR was used to determine the abundance of genes involved in C, N, and P cycling by a SmartChip Real-time PCR system (Wafergen, Fremont, CA, USA) [52]. The protocol contained 66 primer pairs for nutrient-cycling genes (including 35 C-cycling genes, 22 N-cycling genes, and 9 P-cycling genes) and one 16S rRNA gene primer (Table S1). The PCR amplification program followed the following steps. First, an initial denaturation of 95℃ for 10 min, followed by 40 cycles of denaturation at 95℃ for 30 s, followed by annealing at 58℃ for 30 s, and finally an extension at 72℃ for 30 s. The melting curve was automatically generated by the WaferGen software. The relative copy number of the genes was calculated as relative copy number=$10^{(31-CT)/(10/3)}$, where CT represents the threshold cycle [52]. Then, the relative abundance of C-, N-, and P-cycling genes were expressed as copies / 16S rRNA gene.

Microbial carbon substrate utilization and potential enzyme activities

Soil microbial C substrate utilization was assessed as previously published with modifications [53]. It consists of two 96-well microtiter plates placed face to face. Fourteen different substrates, including five amino acids (L-alanine, L-cysteine,

GABA, L-lysine, L-arginine); four carbohydrates (L-arabinose, D-fructose, D-galactose, yrehalose); four carboxylic acids (α-ketoglutaric acid, citric acid, L-malic acid, oxalic acid); one aromatic acid; and ultrapure distilled water (control) were added to four replicates of each soil sample and distributed to microtiter plates. The indicator plates were measured at 570 nm with a plate reader, before and after incubation for 6 hours in the dark (Anthos 2010, Biochrom, Cambridge, UK). The C substrate utilization was calculated from the difference in CO_2 concentration between two measurement times and expressed as μg CO_2-C g^{-1} soil h^{-1}.

Potential enzyme activities, including β-glucosidase, cellobiohydrolase, N-acetyl-β-D-glucosaminidase, leucine-aminopeptidase, acid phosphatase, phenoloxidase and peroxidase enzymes, were measured using a combination of fluorometric and photometric assays [54–56]. 2.0 g of fresh soil was dissolved in 100 mL of 100 mM sodium acetate buffer. 200 μL aliquots of soil suspension were placed into 96-well plates, after which corresponding fluorescence-labeled substrates (Sigma Aldrich, CA, USA) were added. After incubation for 140 min, fluorescence intensity was measured by FLUO star Omega (BMG Labtech, Offenburg, Germany) with 365 nm excitation and 450 nm emission. Potential enzyme activities were then calculated according to the standard curve and expressed in nmol 4-methylumbelliferone (MUF) or 7-amino-4-methylcoumarin (AMC) g^{-1} dry soil h^{-1}. Potential phenoloxidase and peroxidase enzyme activities were measured using 1 mL soil suspensions mixed with

1 mL 20 mM L-3,4-dihydroxyphenylalanine (DOPA) (Sigma Aldrich, CA, USA) as substrate. For peroxidase activity measurements, samples received 10 µL 0.3% (v/v) H_2O_2 as the additional substrate. Absorbance was measured at 450 nm with FLUO star Omega (BMG Labtech, Offenburg, Germany) after shaking and centrifuging before and after 20 hours of incubation. The potential oxidative enzyme activities were calculated from the difference in absorbance between two times and expressed in nmol DOPA g^{-1} dry soil h^{-1}.

Data analyses

For microbial characteristics, nutrient-related gene abundances, enzyme activities, and microbial C utilization, we calculated response ratios (RR) as the ratio between samples that received glucose and samples that did not receive glucose. Differences in soil properties and the RR of the microbial characteristics, nutrient-related gene abundances, enzyme activities, and microbial C utilization between treatments were identified by ANOVA with post hoc tests where appropriate, with $p < 0.05$ considered statistically significant. Repeated-measures ANOVA was used to test the main and interactive effects of glucose addition and incubation time on the cumulative SOM derived CO_2, and three-way ANOVA was used to test the effect of plant species, N addition and P addition on the cumulative PE. A Spearman correlation, followed by post hoc tests, and the Mantel test were used to investigate the relationship between priming effects and soil properties, the RR of microbial communities, nutrient-related

gene abundance, enzyme activities, and microbial C utilization after incubation. The RR of bacterial and fungal communities was calculated as the absolute value of the difference in microbial taxa abundance between the control and glucose treatment. Principal co-ordinates analysis (PCoA) was performed to investigate the effect of plant species and field N and P treatments on the responses of bacterial and fungal communities. Structural equation modeling (SEM) was used to investigate the direct and indirect roles of soil N and P concentrations, microbial biomass, microbial diversity, enzyme activities, microbial C utilization, and nutrient-related gene abundance in driving the priming effect. All statistical analyses were performed using the R platform (version 4.2.2) and the online tool of the Majorbio Cloud Platform (https://cloud.majorbio.com/page/tools/).

Results

SOM-derived CO_2 and SOM priming effect

Our results show that glucose addition had a significant impact on the cumulative CO_2 flux derived from SOM, suggesting a positive priming effect (PE) beneath both leguminous plants (LP) or non-leguminous plants (NLP) (Fig. 1). Further, P alone treatments significantly impacted cumulative priming at the end of the incubation in LP soil. Specifically, NP addition induced the highest priming effect in the NLP

plantation, while the addition of NP and P alone resulted in stronger priming effects than the CK and N treatments for LP.

Soil microorganism responses to field and incubation treatments

As expected, prior to lab incubation, plant species and field nutrient addition significantly influenced both bacterial and fungal community compositions (Fig. S4). After incubations, microbial community responses to glucose addition (response ratios, RR) also significantly differed by dominant plant species and nutrient addition (Fig. 2). Specifically, principal coordinate analysis (PCoA) showed that the profiles of bacterial and fungal communities from different plant soils formed clusters (Fig.2, ANOSIM < 0.05). Further, community similarity analysis revealed significant differences in both bacterial and fungal communities among different nutrient treatments in both plant soils (Fig.2). In addition, bacterial ^{13}C biomass was higher in the NLP plantation than in the LP plantation and bacterial and fungal ^{13}C biomass significantly increased with P addition (Table 2). Plant species identity also significantly affected the RR of bacterial and fungal biomass to priming. The RR of the bacterial and fungal diversity and fungal biomass was significantly different within the P treatment (Table 2).

Factors involved in SOM priming effects

Soil physicochemical and microbial properties showed different responses to chronic field treatments, where P addition appeared to have a greater effect on these basic soil properties (Table 1). While the strength of the priming effect was significantly positively correlated with consumed N and soil P concentration, as well as the bacterial and fungal biomass (Fig. 3A, Fig. S7, and Fig. S8). In addition, the RR of microbial C utilization, nutrient-related gene abundance, and enzyme activities showed different responses to the plant identity and nutrient addition (Table. S2, Fig. S5, and Fig. S6). For instance, C cycling genes are highly expressed in the NP treatment in the NLP stands and in both P and NP treatments in the LP stand (Table. S2). These results match the cases where significant priming effects were observed in our study. Correspondingly, significant positive correlations were found between the priming effect and the RR of nutrient-related gene expression, enzyme activities, and microbial C utilization (Fig. 3 and Fig. S9). Similarly, some microbial taxa also showed convergent patterns of variation with priming, leading to significant correlations between the priming effect and the RRs of the *Proteobacteria*, *Acidobacteria*, and *Actinobacteria* in our results (Fig. S10). Structural equation models (SEM) suggest that soil N and P concentrations affect PE indirectly by altering the microbial community, predominantly by influencing the proportion of nutrient-related genes, increasing carbon utilization, and promoting enzyme activity. (Fig. S11).

Discussion

Nutritional balance regulates the priming effects

Our results demonstrate that dominant plant species identity and long-term nutrient additions both altered soil and microbial properties in subtropical forest soils, and that these changes contributed SOM's susceptibility to decomposition after labile C input. Glucose addition resulted in increased SOM decomposition regardless of dominant overstory plant type or nutrient addition, an effect that can be attributed to "microbial co-metabolism", where microorganisms in soil are C-starved and a proportion of living microbes remain inactive [57, 58]. The addition of labile C triggers microbial activation, enhancing their capacity to decompose SOM [3, 17, 59]. Our findings demonstrate this effect in that glucose addition increased microbial biomass, activity, and SOC utilization, resulting in increased CO_2 release from SOM and a positive priming effect.

Considerable work has proven soil nutrient condition influences SOM decomposition [60–62]. At our study site, long-term P treatment showed a stronger effect on microbial community and priming than N treatment. This is unsurprising, as tropical and subtropical forests are often nutrient-limited due to extreme weathering and highly acidic soils that promote cation bridging and the adsorption of P [25, 29]. Thus, low P availability could restrict microbial biomass and activity [63, 64], and its addition should have more profound effects on the microbial community than N

addition in these systems. While this pattern generally held in our study, interestingly, we found that adding P alone significantly increased the priming effect in the LP soil, but not in the NLP soil. This is likely due to the association of free-living N-fixing microbes that can supply additional N to maintain microbial activity [39, 40]. As a consequence, when LP plantations are supplemented by phosphorus, they are capable of relying on their belowground mutualists to meet a growing need for N. In NLP plantations, however, this P supplementation may simply cause plants to be N-limited, which may explain why P supplementation was not sufficient to increase the priming effect.

Our results show that the combination of N and P addition induced greater CO_2 release from SOM and that combined nutrient addition increased the positive influence of priming in both plantation soils. Balanced and sufficient nutrient availability likely stimulates SOM degradation due to the increased potential decomposition capacity of microorganisms [11]. Balanced nutrient needs lead to a healthier soil microbial community, which in turn leads to the promotion of hydrolytic enzymes that degrade SOM [11, 65]. This premise is consistent with our understanding of nutrient limitation theory. For optimal metabolism and growth of microorganisms, N and P availability would determine microbial metabolism and growth as nutrient demand increases of microbes that got activated through labile C inputs. [27, 61]. This may be particularly true in the tropics, where suggested that soil

N and P availability act together to affect the SOM dynamics through their effect on soil microorganisms[66]. In this fashion, the microbial decomposition of SOM and the ensuing priming effect follows Sprengel-Liebig's Law of the Minimum [28]. In this case, labile carbon does not limit decomposition, but rather levels of essential soil nutrients like nitrogen and phosphorus. This premise is consistent with our observations, such as we found that the positive priming effects in our results, as well as the increased microbial biomass, extracellular enzyme activity, and the abundance of genes involved in nutrient cycling. This suggests that microbial health and nutrient limitation is a crucial components influencing the strength of priming. Correspondingly, we observed higher levels of P and soil N induced a relatively high soil priming effect, and resulted in a relatively lower SOC than fields without NP addition.

Microbial mechanisms underpinning priming effects

Soil microorganisms play a crucial role in priming and are the main agents of SOM decomposition [67]. Several studies have established that soil priming is impacted by variations in microbial biomass and community structure, suggesting that the abiotic influence of soil nutrient conditions indirectly influences SOM decomposition [18, 68, 69]. Similarly, our study found plant species and long-term nutrient addition significantly changed microbial community composition, and these changes in microbial community composition influenced soil priming. For example, the response

ratio of microbial biomass was significantly correlated with the measured priming effect. In addition, we found that soil communities in plantations with artificial nutrient addition responded differently to exogenous glucose supplementation than in unfertilized plantations. Our results also show a positive correlation between the priming effect and the response ratio of the abundance of *Proteobacteria* and *Acidobacteria*, which have been found to be closely associated with litter decomposition and SOM mineralization [19, 70]. Similar results were also found the significant correlation between the priming effect and microbial taxa composition in other recent studies [69, 71].

In our study, glucose addition increased the abundance of nutrient-related cycling genes, and the strength of the priming effect was positively correlated with the RR of the abundance of genes involved in nutrient cycling. These results suggest that microbial communities may enhance their utilization of soil organic C by altering the abundance of genes involved in SOM decomposition after receiving labile C inputs. High levels of expression in microbial functional genes suggest a commensurately high production of extracellular enzymes necessary for microbial organic C utilization and SOM decomposition [72, 73]. Generally, soil organic matter can be utilized by microorganisms only after it has been converted into smaller substances by enzymatic degradation [69, 74]. We observed that the input of labile C promotes the production of the enzymes involved in the mineralization of SOM. This is consistent with our

understanding of microbial SOM decomposition that the variation in the abundance of the microbial functional genes can be reflected in specific extracellular enzyme activities, and there is likely an intimate link between the changes in microbial functional gene abundance and enzyme-mediated soil C dynamics [20]. For instance, a large-scale study in Australia has found a significant correlation between the abundance of microbial functional genes and C-cycling-related enzyme activities [22]. These findings are consistent with our observations. We observed that labile C had the strongest influence on soil priming when microbial communities were least limited by other soil nutrients – such as nitrogen and phosphorus. In these cases, the introduction of glucose (labile C) strongly stimulated microbial biomass, activity, and the relative abundance of genes associated with nutrient cycling. In turn, this activated belowground facilitates positive feedback in SOM, which we understand as priming. Our results suggest that this priming effect was strongest when the microbial community was least limited by nutrient availability – either through natural rhizomatous mutualisms associated with LP plantations or through artificial nutrient addition.

Conclusion

Using a field nutrient-addition experiment together with a lab incubation experiment, we investigated the interaction between plant physiology and long-term N and P addition affect SOM priming and its drivers in a subtropical forest. We found that the

input of labile C enhanced the SOM decomposition and reduced soil carbon storage potential by increasing soil microbial activity and community composition, especially when the soil has a balanced and sufficient N and P availability. In addition, soil priming was co-limited by N and P in non-legume soils, whereas priming was limited by P only due to the additional N supplied by N-fixing rhizobia in legume soils. Moreover, our study highlights the role of the interaction between plant physiology and soil nutrient availability in affecting the abundance of microbial genes and enzyme activities involved in soil nutrient cycling, which in turn drives the microbial utilization of soil organic C and determines the priming effect in this forest ecosystem. Overall, this study provides novel insights into our understanding of the functional effects of microbial communities on the soil priming effect and highlights how the interaction between plant and nutrient balance can impact SOM priming.

Conflict of interest

The authors declare that they have no conflict of interest.

Acknowledgments

JL was supported by the National Natural Science Foundation of China (42207262 and 42177289) and the China Postdoctoral Science Foundation (2021M703135). JS was supported by Spanish Government grant. JP and JS were supported by the Spanish Government grants PID2020-115770RB-I00 and TED2021-132627B-I00 funded by MCIN, AEI/10.13039/501100011033 and the European NextGenerationEU/PRTR, the Fundación Ramón Areces grant CIVP20A6621, and the Catalan government project SGR2021-01333.

Data Availability Statement

The sequencing raw data are deposited in the NCBI Short Read Archive database under accession numbers PRJNA884088 and PRJNA884089.

References

1. Davidson EA, Janssens IA. Temperature sensitivity of soil carbon decomposition and feedbacks to climate change. Nature. 2006; **440**: 165–173.
2. Lal R. Digging deeper: A holistic perspective of factors affecting soil organic carbon sequestration in agroecosystems. Glob Change Biol. 2018; **24**: 3285–3301.
3. Li J, Alaei S, Zhou MY, Bengtson P. Root influence on soil nitrogen availability and microbial community dynamics results in contrasting rhizosphere priming effects in pine and spruce soil. Funct Ecol. 2021; **35**: 1312–1324.
4. Rasul M, Cho J, Shin HS, Hur J. Biochar-induced priming effects in soil via modifying the status of soil organic matter and microflora: A review. Sci Total Environ. 2022; **805**: 150304.

5. Cheng WX. Rhizosphere feedbacks in elevated CO_2. Tree Physiol. 1999; **19**: 313–320.

6. Kuzyakov Y, Friedel JK, Stahr K. Review of mechanisms and quantification of priming effects. Soil Biol Biochem. 2000; **32**: 1485–1498.

7. Bastida F, García C, Fierer N, Eldridge DJ, Bowker MA, Abades S, et al. Global ecological predictors of the soil priming effect. Nat Commun. 2019; **10**: 1–9.

8. Huo CF, Luo YQ, Cheng WX. Rhizosphere priming effect: A meta-analysis. Soil Biol Biochem. 2017; **111**: 78–84.

9. Guenet B, Camino-Serrano M, Ciais P, Tifafi M, Maignan F, Soong JL, et al. Impact of priming on global soil carbon stocks. Glob Change Biol. 2018; **24**: 1873–1883.

10. Morrissey EM, Mau RL, Schwartz E, McHugh TA, Dijkstra P, Koch BJ, et al. Bacterial carbon use plasticity, phylogenetic diversity and the priming of soil organic matter. ISME J. 2017; **11**: 1890–1899.

11. Chen RR, Senbayram M, Blagodatsky S, Myachina O, Dittert K, Lin XG, et al. Soil C and N availability determine the priming effect: microbial N mining and stoichiometric decomposition theories. Global Change Biol. 2014; **20**: 2356–2367.

12. Feng J, Zhu B. Global patterns and associated drivers of priming effect in response to nutrient addition. Soil Biol Biochem. 2021; **153**: 108118.

13. Li J, Zhou M, Alaei S, Bengtson P. Rhizosphere priming effects differ between Norway spruce (Picea abies) and Scots pine seedlings cultivated under two levels of light intensity. Soil Biol Biochem. 2020; **145**: 107788.

14. Li J, Bengtson P. Comparative analysis of planted and unplanted controls for assessment of rhizosphere priming effect. Pedosphere. 2022; **32**: 884–892.

15. Liu XJA, Finley BK, Mau RL, Schwartz E, Hungate BA. The soil priming effect: Consistent across ecosystems, elusive mechanisms. Soil Biol Biochem 2020; **140**: 107617.

16. Blagodatskaya E, Kuzyakov Y. Mechanisms of real and apparent priming effects and their dependence on soil microbial biomass and community structure: critical review. Biol Fertil Soils. 2008; **45**: 115–131.

17. Lv C, Wang C, Cai A, Zhou Z. Global magnitude of rhizosphere effects on soil microbial communities and carbon cycling in natural terrestrial ecosystems. Sci Total Environ. 2022; **856**: 158961.

18. Razanamalala K, Razafimbelo T, Maron P-A, Ranjard L, Chemidlin N, Lelièvre M, et al. Soil microbial diversity drives the priming effect along climate gradients: a case study in Madagascar. ISME J. 2018; **12**: 451–462.

19. Tao X, Feng J, Yang Y, Wang G, Tian R, Fan F, et al. Winter warming in Alaska accelerates lignin decomposition contributed by Proteobacteria. Microbiome. 2020; **8**: 1–12.

20. Chen J, Sinsabaugh RL. Linking microbial functional gene abundance and soil extracellular enzyme activity: Implications for soil carbon dynamics. Glob Chang Biol. 2021; **27**: 1322–1325.

21. Manoharan L, Kushwaha SK, Ahrén D, Hedlund K. Agricultural land use determines functional genetic diversity of soil microbial communities. Soil Biol Biochem. 2017; **115**: 423–432.

22. Trivedi P, Delgado-Baquerizo M, Trivedi C, Hu H, Anderson IC, Jeffries TC, et al. Microbial regulation of the soil carbon cycle: evidence from gene–enzyme relationships. ISME J. 2016; **10**: 2593–2604.

23. Zhao F, Wang J, Li Y, Xu X, He L, Wang J, et al. Microbial functional genes driving the positive priming effect in forest soils along an elevation gradient. Soil Biol Biochem. 2022; **165**: 108498.

24. Song M, Guo Y, Yu F, Zhang X, Cao G, Cornelissen JHC. Shifts in priming partly explain impacts of long-term nitrogen input in different chemical forms on soil organic carbon storage. Glob Chang Biol. 2018; **24**: 4160-4172.

25. Fang XM, Zhang XL, Chen FS, Zong YY, Bu W-S, Wan S-Z, et al. Phosphorus addition alters the response of soil organic carbon decomposition to nitrogen deposition in a subtropical forest. Soil Biol Biochem. 2019; **133**: 119-128.

26. Liu W, Qiao C, Yang S, Bai W, Liu L. Microbial carbon use efficiency and priming effect regulate soil carbon storage under nitrogen deposition by slowing soil organic matter decomposition. Geoderma. 2018; **332**: 37–44.

27. Hessen DO. Carbon sequestration in ecosystems: the role of stoichiometry. Ecology. 2004; **85**: 1179–1192.

28. Liebig JF. Animal Chemistry: Or, Organic chemistry in its applications to physiology and pathology. 1842. Johnson Reprint Corporation, New York, USA.

29. Camenzind T, Hättenschwiler S, Treseder KK, Lehmann A, Rillig MC. Nutrient limitation of soil microbial processes in tropical forests. Ecol Monogr. 2018; **88**: 4-21.

30. Jobbágy EG, Jackson RB. The vertical distribution of soil organic carbon and its relation to climate and vegetation. Ecol Appl. 2000; **10**: 423–436.

31. Schulte-Uebbing L, de Vries W. Global-scale impacts of nitrogen deposition on tree carbon sequestration in tropical, temperate, and boreal forests: A meta-analysis. Glob Change Biol. 2018; **24**: e416–e431.

615 32. Vitousek PM, Porder S, Houlton BZ, Chadwick OA. Terrestrial phosphorus limitation:
616 mechanisms, implications, and nitrogen-phosphorus interactions. Ecol Appl. 2010; **20**:
617 5–15.

618 33. Du E, Fenn ME, De Vries W, Ok YS. Atmospheric nitrogen deposition to global
619 forests: Status, impacts and management options. Envion Pollut. 2019; **250**: 1044-1048.

620 34. Elrys AS, Zhu Q, Jiang C, Liu J, Sobhy HHH, Shen Q, et al. Global soil nitrogen cycle
621 pattern and nitrogen enrichment effects: Tropical versus subtropical forests. Glob Chang
622 Biol. 2023; **29**: 1905–1921.

623 35. Elser JJ, Bracken ME, Cleland EE, Gruner DS, Harpole WS, Hillebrand H, et al. Global
624 analysis of nitrogen and phosphorus limitation of primary producers in freshwater,
625 marine and terrestrial ecosystems. Ecol Lett. 2007; **10**: 1135–1142.

626 36. Wang S, Zhou K, Mori T, Mo J, Zhang W. Effects of phosphorus and nitrogen
627 fertilization on soil arylsulfatase activity and sulfur availability of two tropical
628 plantations in southern China. For Ecol Manage. 2019; **453**: 117316.

629 37. Lu J, Yang J, Keitel C, Yin L, Wang P, Cheng W, et al. Rhizosphere priming effects of
630 Lolium perenne and Trifolium repens depend on phosphorus fertilization and biological
631 nitrogen fixation. Soil Biol Biochem. 2020; **150**: 108005.

632 38. Phillips RP, Fahey TJ. Tree species and mycorrhizal associations influence the
633 magnitude of rhizosphere effects. Ecology. 2006; **87**: 1302–1313.

634 39. Bhattacharyya PN, Jha DK. Plant growth-promoting rhizobacteria (PGPR): emergence
635 in agriculture. World J Microbiol Biotechnol 2012; **28**: 1327–1350.

636 40. Kawaka F. Characterization of symbiotic and nitrogen fixing bacteria. AMB Express.
637 2022; **12**: 1–11.

638 41. Zhang W, Zhu X, Luo Y, Rafique R, Chen H, Huang J, et al. Responses of nitrous oxide
639 emissions to nitrogen and phosphorus additions in two tropical plantations with N-
640 fixing vs. non-N-fixing tree species. Biogeosci Disc. 2014; **11**: 1413–1442.

641 42. Hicks LC, Leizeaga A, Rousk K, Michelsen A, Rousk J. Simulated rhizosphere deposits
642 induce microbial N-mining that may accelerate shrubification in the subarctic. Ecology.
643 2020; **101**.

644 43. Rousk J, Smith AR, Jones DL. Investigating the long-term legacy of drought and
645 warming on the soil microbial community across five European shrubland ecosystems.
646 Glob Chang Biol. 2013; **19**: 3872–84.

647 44. RK. Lu. Analytical Methods of Soil Agrochemistry. Chinese Agriculture Science and
648 Technology Press, Beijing 1999.

649 45. Brookes PC, Landman A, Pruden G, Jenkinson DS. Chloroform fumigation and the
650 release of soil-nitrogen-a rapid direct extraction method to measure microbial biomass
651 nitrogen in soil. Soil Biol Biochem. 1985; **17**: 837–842.

652 46. Frostegård Å, Bååth E, Tunlio A. Shifts in the structure of soil microbial communities
653 in limed forests as revealed by phospholipid fatty acid analysis. Soil Biol Biochem.
654 1993; **25**: 723–730.

655 47. Dumont MG, Murrell JC. Stable isotope probing-linking microbial identity to function.
656 Nat Rev Microbiol. 2005; **3**: 499–504.

657 48. Zhang K, Ni Y, Liu X, Chu H. Microbes changed their carbon use strategy to regulate
658 the priming effect in an 11-year nitrogen addition experiment in grassland. Sci Total
659 Environ. 2020; **727**: 138645.

660 49. Neufeld JD, Vohra J, Dumont MG, Lueders T, Manefield M, Friedrich MW, et al. DNA
661 stable-isotope probing. Nat Protoc. 2007; **2**: 860–866.

662 50. Zhou J, Deng Y, Luo F, He Z, Yang Y. Phylogenetic molecular ecological network of
663 soil microbial communities in response to elevated CO_2. MBio. 2011; **2**: e00122-11.

664 51. Ihrmark K, Bödeker I, Cruz-Martinez K, Friberg H, Kubartova A, Schenck J, et al. New
665 primers to amplify the fungal ITS2 region–evaluation by 454-sequencing of artificial
666 and natural communities. FEMS Microbiol Ecol. 2012; **82**: 666–677.

667 52. Zheng B, Zhu Y, Sardans J, Penuelas J, Su J. QMEC: a tool for high-throughput
668 quantitative assessment of microbial functional potential in C, N, P, and S
669 biogeochemical cycling. Science China Life Sciences. 2018; **61**: 1451–1462.

670 53. Campbell CD, Chapman SJ, Cameron CM, Davidson MS, Potts JM. A rapid microtiter
671 plate method to measure carbon dioxide evolved from carbon substrate amendments so
672 as to determine the physiological profiles of soil microbial communities by using whole
673 soil. Appl Environ Microbiol. 2003; **69**: 3593–3599.

674 54. Marx MC, Wood M, Jarvis SC. A microplate fluorimetric assay for the study of enzyme
675 diversity in soils. Soil Biol Biochem. 2001; **33**: 1633–1640.

676 55. Saiya-Cork KR, Sinsabaugh RL, Zak DR. The effects of long term nitrogen deposition
677 on extracellular enzyme activity in an Acer saccharum forest soil. Soil Biol Biochem.
678 2002; **34**: 1309–1315.

679 56. Wild B, Li J, Pihlblad J, Bengtson P, Rütting T. Decoupling of priming and microbial N
680 mining during a short-term soil incubation. Soil Biol Biochem. 2018; **129**: 71–79.

681 57. Heuck C, Weig A, Spohn M. Soil microbial biomass C: N: P stoichiometry and
682 microbial use of organic phosphorus. Soil Biol Biochem. 2015; **85**: 119–129.

683 58. Widdig M, Schleuss P-M, Biederman LA, Borer ET, Crawley MJ, Kirkman KP, et al.
684 Microbial carbon use efficiency in grassland soils subjected to nitrogen and phosphorus
685 additions. Soil Biol Biochem. 2020; **146**: 107815.

686 59. Kuzyakov, Blagodatskaya E. Microbial hotspots and hot moments in soil: concept and
687 review. Soil Biol Biochem. 2015; **83**: 184–199.

688 60. Bei S, Li X, Kuyper TW, Chadwick DR, Zhang J. Nitrogen availability mediates the
689 priming effect of soil organic matter by preferentially altering the straw carbon-
690 assimilating microbial community. Sci Total Environ. 2022; **815**: 152882.

691 61. Mehnaz KR, Corneo PE, Keitel C, Dijkstra FA. Carbon and phosphorus addition effects
692 on microbial carbon use efficiency, soil organic matter priming, gross nitrogen
693 mineralization and nitrous oxide emission from soil. Soil Biol Biochem. 2019; **134**:
694 175–186.

695 62. Wu W, Wang F, Xia A, Zhang Z, Wang Z, Wang K, et al. Meta-analysis of the impacts
696 of phosphorus addition on soil microbes. Agric, Ecosyst Environ. 2022; **340**: 108180.

697 63. Ilstedt U, Giesler R, Nordgren A, Malmer A. Changes in soil chemical and microbial
698 properties after a wildfire in a tropical rainforest in Sabah, Malaysia. Soil Biol Biochem.
699 2003; **35**: 1071–1078.

700 64. Jing Z, Chen R, Wei S, Feng Y, Zhang J, Lin X. Response and feedback of C
701 mineralization to P availability driven by soil microorganisms. Soil Biol Biochem.
702 2017; **105**: 111–120.

703 65. Zhu Z, Ge T, Luo Y, Liu S, Xu X, Tong C, et al. Microbial stoichiometric flexibility
704 regulates rice straw mineralization and its priming effect in paddy soil. Soil Biol
705 Biochem. 2018; **121**: 67–76.

706 66. Ilstedt, Singh S. Nitrogen and phosphorus limitations of microbial respiration in a
707 tropical phosphorus-fixing acrisol (ultisol) compared with organic compost. Soil Biol
708 Biochem. 2005; **37**: 1407–1410.

709 67. Delgado-Baquerizo M, Maestre FT, Reich PB, Jeffries TC, Gaitan JJ, Encinar D, et al.
710 Microbial diversity drives multifunctionality in terrestrial ecosystems. Nat Commun.
711 2016; **7**: 10541.

712 68. Fu X, Song Q, Li S, Shen Y, Yue S. Dynamic changes in bacterial community structure
713 are associated with distinct priming effect patterns. Soil Biol Biochem. 2022; **169**:
714 108671.

715 69. Zhou S, Wang J, Chen L, Wang J, Zhao F. Microbial community structure and
716 functional genes drive soil priming effect following afforestation. Sci Total Environ.
717 2022; **825**: 153925.

718 70. Blagodatskaya, Khomyakov N, Myachina O, Bogomolova I, Blagodatsky S, Kuzyakov
719 Y. Microbial interactions affect sources of priming induced by cellulose. Soil Biol
720 Biochem. 2014; **74**: 39–49.

721 71. Yang H, Li Y, Wang S, Zhan J, Ning Z, Han D. The Response of critical microbial taxa
722 to litter micro-nutrients and macro-chemistry determined the agricultural soil priming
723 intensity after afforestation. Front Microbiol. 2021; **12**: 730117.

724 72. Xiao W, Chen X, Jing X, Zhu B. A meta-analysis of soil extracellular enzyme activities
725 in response to global change. Soil Biol Biochem. 2018; **123**: 21–32.

726 73. Zechmeister-Boltenstern S, Keiblinger KM, Mooshammer M, Peñuelas J, Richter A,
727 Sardans J, et al. The application of ecological stoichiometry to plant–microbial–soil
728 organic matter transformations. Ecol Monogr. 2015; **85**: 133–155.

729 74. Lehmann J, Kleber M. The contentious nature of soil organic matter. Nature. 2015; **528**:
730 60–68.

731

732 Table 1. Soil and microbial characteristics.

		Soil pH	SOC (gkg^{-1})	TN (gkg^{-1})	TP (gkg^{-1})	AP ($mgkg^{-1}$)	IN_{begin} ($mgkg^{-1}$)	IN_{end} ($mgkg^{-1}$)	$IN_{consumed}$ ($mgkg^{-1}$)	Soil C: N	Soil C: P	Soil N: P	MBC (mgg^{-1})	MBN (mgg^{-1})
Non-Leguminous Plants	CK	3.8±0.1ab	19±1.0a	1.4±0.1a	0.2±0.1a	0.2±0.1a	16.6±0.6a	2.9±0.3a	13.7±0.9a	13.7±0.9a	9.0±1.3a	125±26a	0.8±0.2a	0.1±0.1a
	N	3.6±0.1b	20.0±1.5a	1.4±0.1a	0.2±0.1a	0.2±0.1a	20.1±1.9b	5.5±0.8b	14.7±1.2ab	14.0±0.9a	10.7±2.4a	152±40a	0.7±0.1a	0.2±0.1ab
	P	3.8±0.1a	18.0±1.5a	1.3±0.1a	0.5±0.1b	47.8±2.6b	15.9±1.1a	2.4±0.3a	13.5±0.8a	13.7±0.5a	2.9±0.3b	40±5b	0.9±0.2a	0.2±0.1b
	NP	3.6±0.1ab	16.0±2.8a	1.3±0.1a	0.5±0.1b	46.3±1.1b	22.7±0.8b	3.0±0.1a	17.7±0.8b	12.4±2.0a	3.0±0.5b	35±5b	0.8±0.1a	0.2±0.1ab
Leguminous Plants	CK	3.7±0.1ab	27.1±1.0a	1.9±0.1a	0.2±0.1a	0.4±0.1a	18.2±1.6ab	4.8±1.1a	13.4±0.6a	14.2±0.1a	12.0±2.0a	171±28a	1.9±0.2a	0.2±0.1a
	N	3.6±0.1a	27.0±2.4a	1.9±0.2a	0.1±0.1a	0.4±0.1a	21.2±3.6a	8.3±2.0b	12.9±1.7a	14.4±0.4a	15.4±2.3a	220±30a	1.7±0.2a	0.2±0.1a
	P	3.8±0.1b	22.2±2.0ab	1.7±0.1ab	0.4±0.1b	46.1±4.3b	17.1±2.0b	2.6±0.3a	14.5±1.8a	13.4±0.6a	4.4±1.1b	59±15b	1.3±0.1a	0.1±0.1ab
	NP	3.6±0.1a	20.0±0.8a	1.5±0.1b	0.5±0.1b	57.8±4.0c	21.6±0.4a	3.0±0.4a	18.6±0.6b	13.4±0.2a	3.0±0.3b	40±3b	1.4±0.2a	0.1±0.1b
ANOVA *p*	S	n.s.	*	***	n.s.	n.s.	n.s.	*	n.s.	n.s.	*	*	***	n.s.
	N	**	n.s.	n.s.	n.s.	n.s.	***	**	**	n.s.	n.s.	n.s.	n.s.	n.s.
	P	n.s.	**	*	***	***	n.s.	***	**	n.s.	***	***	n.s.	n.s.
	SxN	n.s.	n.s.	n.s.	n.s.	n.s.	n.s.	n.s.	n.s.	n.s.	n.s.	n.s.	n.s.	n.s.
	SxP	n.s.	n.s.	*	n.s.	n.s.	n.s.	*	n.s.	n.s.	n.s.	n.s.	n.s.	**
	NxP	n.s.	n.s.	n.s.	n.s.	n.s.	n.s.	*	**	n.s.	n.s.	n.s.	n.s.	n.s.
	SxNxP	n.s.	n.s.	n.s.	n.s.	n.s.	n.s.	n.s.	n.s.	n.s.	n.s.	n.s.	n.s.	n.s.

733 Values are means followed by standard errors (n = 3), where S = species; CK = no nitrogen or phosphorus addition; N = nitrogen addition, P = phosphorus addition, NP = nitrogen and
734 phosphorus addition; SOC = soil organic carbon; TN = total nitrogen; TP = total phosphorus; AP = available phosphorus; IN = inorganic nitrogen in glucose treatments at the beginning and
735 end of the incubations and the amount consumed; MBC=microbial biomass carbon; MBN=microbial biomass nitrogen. Different letters indicate a significant difference between treatments
736 within each plant identity (ANOVA, $P < 0.05$, Tukey's post-hoc analysis). ***: $p < 0.001$,**: $p < 0.01$,*: $p < 0.05$, n.s.: $p > 0.05$.

737 Table 2. Response ratios (RR) of microbial biomass and alpha diversity at the end of the incubation experiment.

		Bacterial ^{13}C biomass (n mol/g)	Fungal ^{13}C biomass (n mol/g)	RR-bacterial biomass	RR- fungal biomass	RR-bacterial Sobs index	RR-bacterial Shannon index	RR-fungal Sobs index	RR-fungal Shannon index
Non-Leguminous Plants	CK	11.8±2.1a	0.7±0.1a	1.5±0.1ac	1.9±0.1a	0.8±0.1a	0.9±0.1a	0.4±0.1a	0.7±0.2a
	N	9.9±0.4a	0.8±0.1ab	1.4±0.1bc	1.9±0.3a	1.0±0.1a	1.0±0.1ab	0.6±0.1b	0.8±0.1a
	P	11.8±0.7a	0.9±0.1ab	1.2±0.1b	2.6±0.4a	1.0±0.1a	1.0±0.1ab	0.5±0.1ab	0.7±0.1a
	NP	13.8±1.5a	1.3±0.2b	1.7±0.1a	2.8±0.3a	1.1±0.2a	1.1±0.1b	0.5±0.1ab	0.7±0.1a
Leguminous Plants	CK	8.2±1.4A	0.7±0.1A	1.2±0.1A	1.5±0.3A	0.9±0.1A	1.0±0.1A	0.6±0.1A	0.9±0.2A
	N	6.0±0.7A	0.7±0.1A	1.2±0.1A	1.8±0.4AB	1.0±0.1AB	1.0±0.1A	0.9±0.3A	0.8±0.1A
	P	9.4±0.8A	1.1±0.1B	1.2±0.1A	2.2±0.1B	1.0±0.2AB	1.0±0.1A	0.4±0.1A	0.6±0.1AB
	NP	9.1±1.1A	1.0±0.2B	1.4±0.1A	2.1±0.2B	1.4±0.1B	1.1±0.1B	0.5±0.1A	0.4±0.1B
ANOVA *p*	S	**	n.s.	**	*	n.s.	n.s.	n.s.	n.s.
	N	n.s.	n.s.	n.s.	n.s.	n.s.	n.s.	n.s.	n.s.
	P	*	**	n.s.	*	n.s.	*	n.s.	*
	SxN	n.s.	n.s.	n.s.	n.s.	n.s.	n.s.	n.s.	n.s.
	SxP	n.s.	n.s.	n.s.	n.s.	n.s.	n.s.	n.s.	*
	NxP	n.s.	n.s.	**	n.s.	n.s.	n.s.	n.s.	n.s.
	SxNxP	n.s.	n.s.	*	n.s.	n.s.	n.s.	n.s.	n.s.

Values are means followed by standard errors (n = 3), where S = species; CK = no nitrogen or phosphorus addition; N = nitrogen addition, P = phosphorus addition, NP = nitrogen and phosphorus addition; and RR is the response ratio comparing glucose treatment and control. Different letters indicate a significant difference between different treatments within each plant identity (ANOVA, $P < 0.05$, Tukey's post-hoc analysis). ***: $p < 0.001$,**: $p < 0.01$,*: $p < 0.05$, n.s.: $p > 0.05$.

Figure legends:

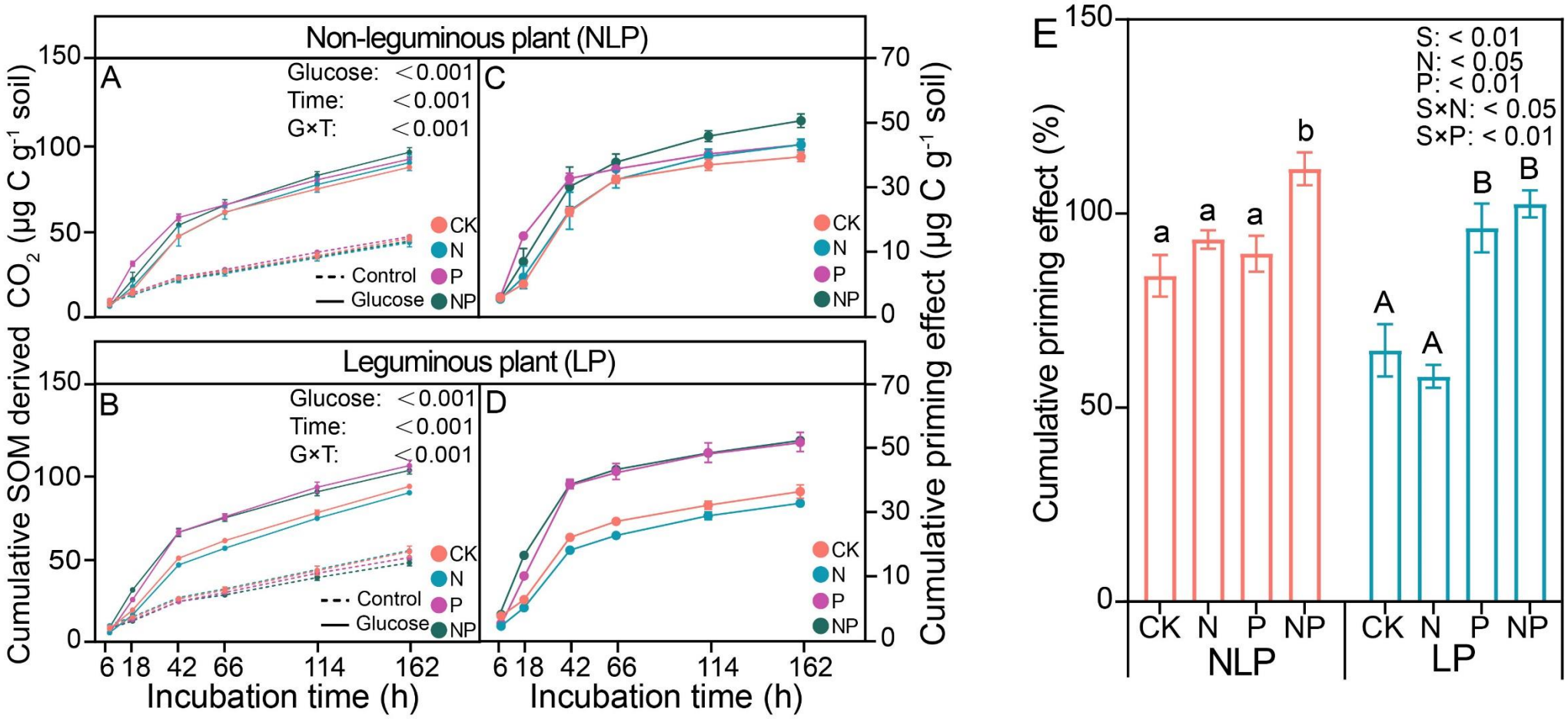

Fig.1. Cumulative SOM-derived CO_2 fluxes (A and B) and priming effects (C and D) by treatment over the course of the incubation, and cumulative priming effects (E) at the end of the incubation (LP = leguminous plant, NP = non-leguminous plant, S = species, CK = no nitrogen or phosphorus addition, N = nitrogen addition, P = phosphorus addition, and NP = nitrogen and phosphorus addition). Different letters indicate significant differences at $P < 0.05$.

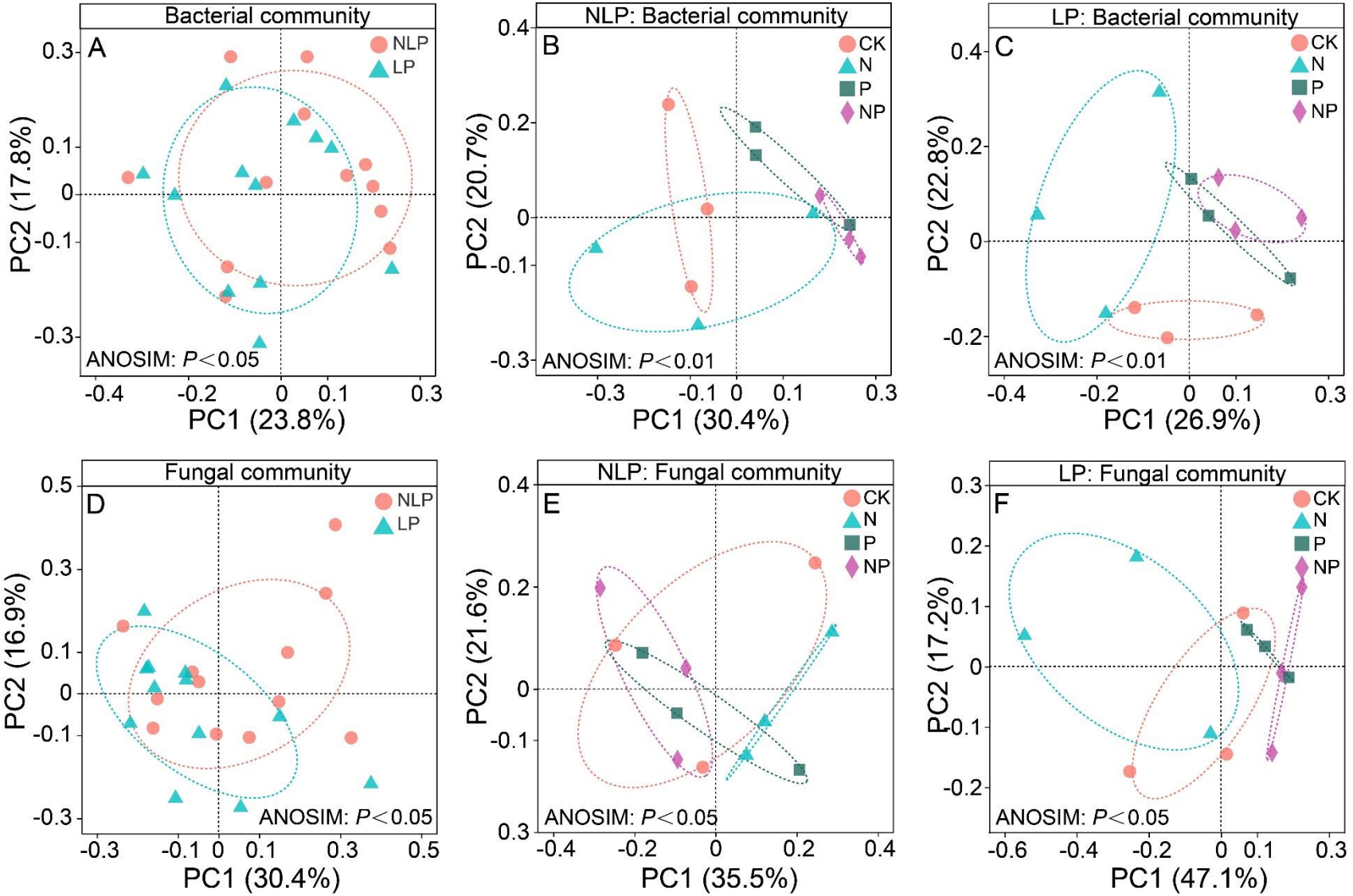

Fig.2. Principal co-ordinates analysis (PCoA) of the response ratio (RR) of bacterial and fungal communities among treatments (LP = leguminous plant, NP = non-leguminous plant, CK = no nitrogen or phosphorus addition, N = nitrogen addition, P = phosphorus addition, and NP = nitrogen and phosphorus addition).

The RR of bacterial and fungal communities was calculated as the variation of the microbial taxa between glucose treatment and control.

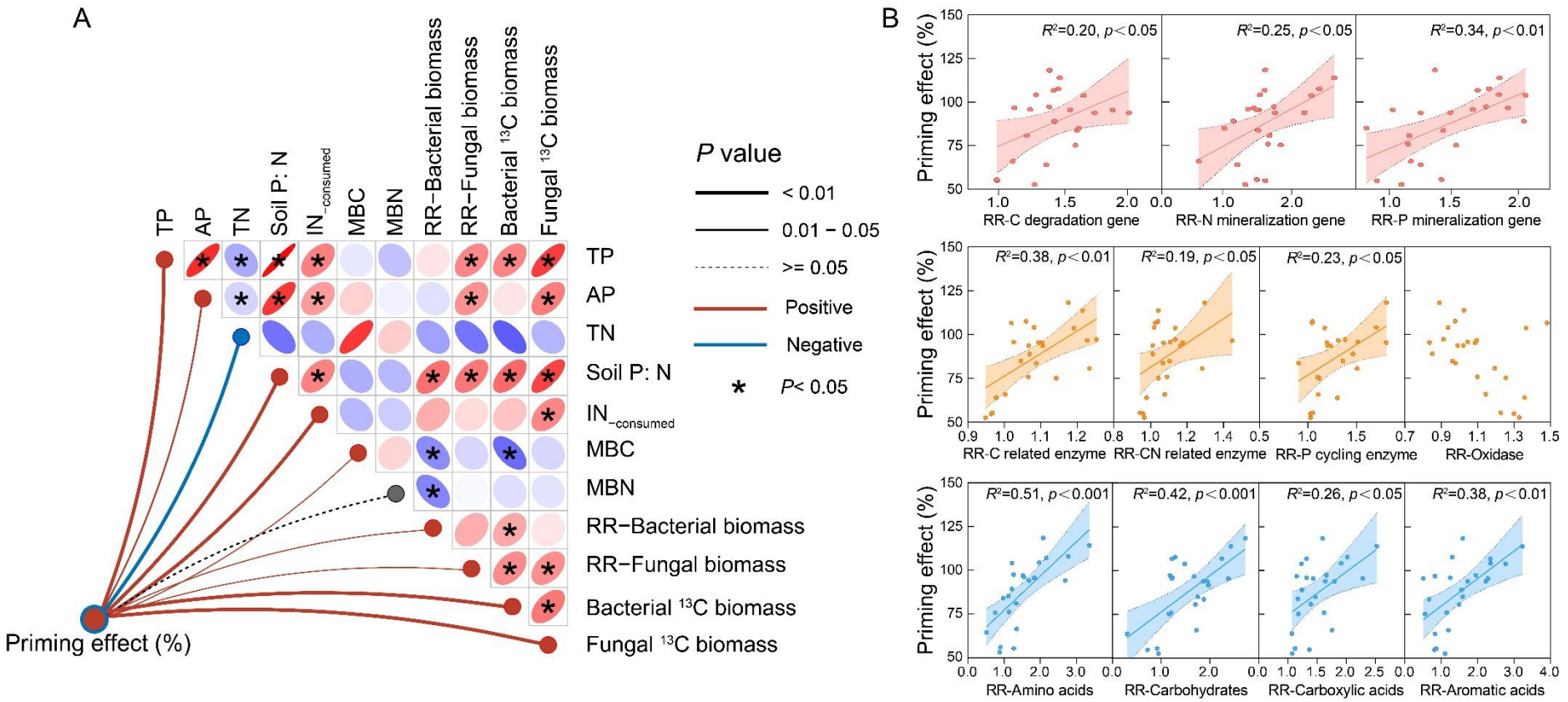

Fig.3. (A) Pearson correlations between the priming effect and microbial community and soil properties. (B) Correlations of priming effects with the response ratios (RR) of carbon utilization, nutrient-cycling gene expression, and enzyme activities after incubation. The RR of the microbial gene expression, enzyme activities, and microbial carbon utilization were calculated by the ratio between control and glucose treatment. TN =

total nitrogen; TP = total phosphorus; AP = available phosphorus; IN = inorganic nitrogen in glucose treatments at the beginning and end of the incubations and the amount consumed; MBC=microbial biomass carbon; MBN=microbial biomass nitrogen.

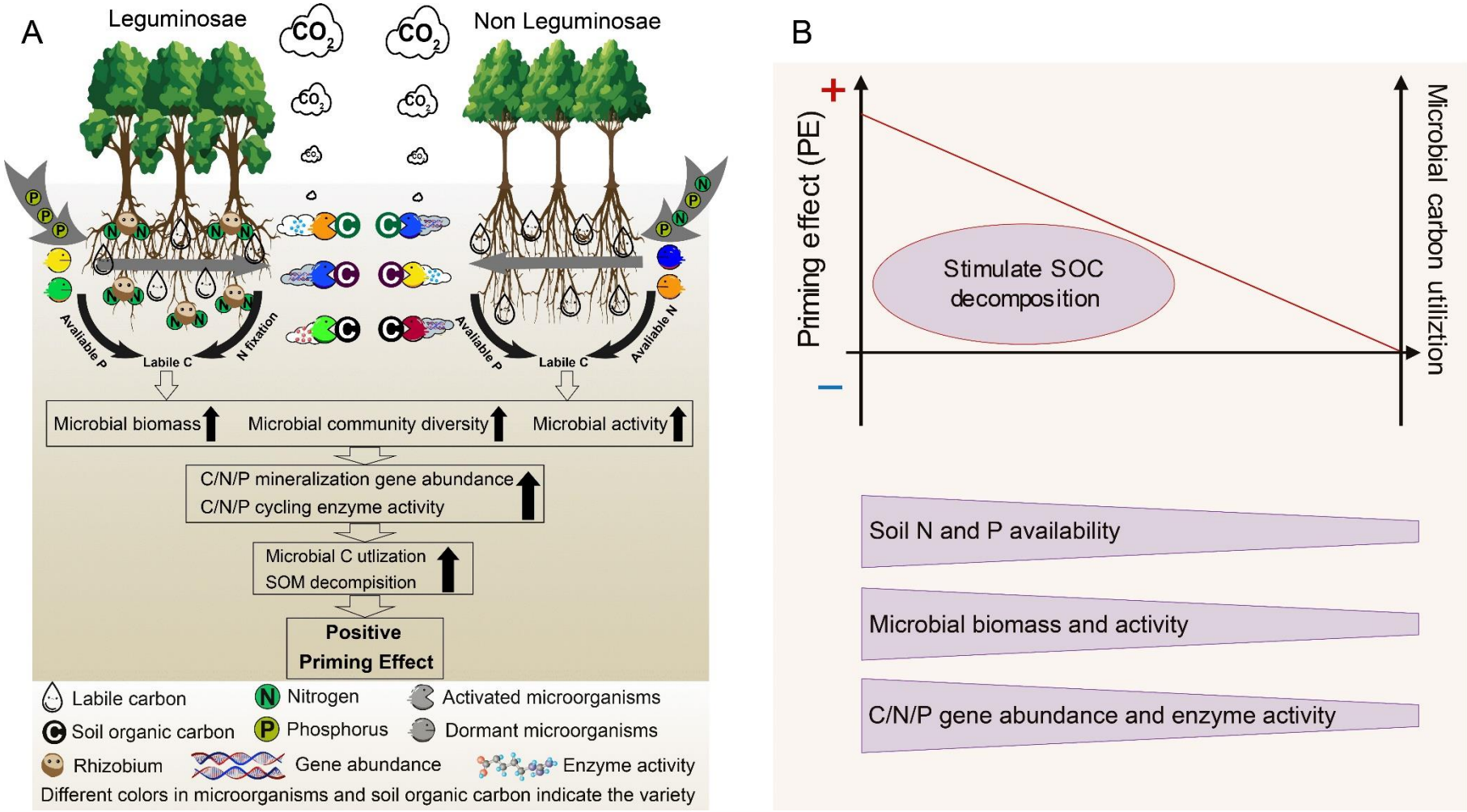

Fig.4. Conceptual diagram depicting factors and mechanisms underlying the soil priming effect. Trapezoid thickness increases as a value of variable increases.

Supporting Information

Table S1. List of primer pairs used in the present study. Bold font indicates the primer pairs with positive results.

Table S2. Response ratio of gene expression, enzyme activities and carbon utilization in different samples.

Table S3. Correlations between the priming effect and microbial community,soil properties, and the response ratios (RR) of carbon utilization, nutrient-cycling gene expression, and enzyme activities after incubation.

Table S4. The path from structural equation models (SEM) of nitrogen (N) or phosphorus (P) addition effect on the priming effect.

Table S5. The standardized path coefficients from structural equation models (SEM) of nitrogen (N) or phosphorus (P) addition effect on the priming effect.

Fig. S1. Schematic diagram of the fertilizer addition plots (CK = no nitrogen or phosphorus addition; N = nitrogen addition, P = phosphorus addition, and NP = nitrogen and phosphorus addition).

Fig. S2. Flow diagram of experimental design and analytical procedures.

Fig. S3. Variation in inorganic nitrogen content during the incubation. Eucalyptus Urophylla (NLP), Acacia Auriculiformis (LP), No nitrogen and phosphorus treatment (CK), Nitrogen treatment (N), Phosphorus treatment (P), Nitrogen and phosphorus treatment (NP).

Fig. S4. PCoA analysis of bacterial and fungal communities prior to incubation experiment (LP = leguminous plant, NP = non-leguminous plant, CK = no nitrogen or

phosphorus addition, N = nitrogen addition, P = phosphorus addition, and NP = nitrogen and phosphorus addition).

Fig. S5. Relationships between response ratios (RR) of microbial community properties, carbon utilization, nutrient cycling gene expression, enzyme activities, and soil properties after incubation. The RR of microbial gene expression, enzyme activities, and microbial carbon utilization were calculated as the ratio between glucose treatment and control.

Fig. S6. Relationships between response ratios (RR) of the microbial community and soil properties after incubation. The RR of the microbial communities were calculated by the variation of the microbial taxa between glucose treatment and control.

Fig. S7. Relationships between SOM priming and soil properties (SOC = soil organic carbon; TN = total nitrogen;TP = total phosphorus,; AP = available phosphorus, and IN = inorganic nitrogen in glucose treatments at the beginning and end of the incubations and the amount of inorganic nitrogen consumed during the incubation.

Fig. S8. Relationships between SOM priming and response ratios (RR) of microbial biomass after incubation. The RR of the microbial properties were calculated by the ratio between glucose treatment and control.

Fig. S9. Relationships between SOM priming and response ratios (RR) of nutrient cycling gene expression after incubation. The RR of the microbial gene expression were calculated by the ratio between glucose treatment and control.

Fig. S10. Relationships between the priming effect and response ratios (RR) of the microbial community. The RR of the microbial communities were calculated by the variation of the microbial taxa between glucose treatment and control.

Fig. S11. Path diagrams (A) and standardized path coefficients (B) from structural equation models (SEM) of the priming effect. Solid arrows indicate significant relationships ($p < 0.05$) and dashed arrows indicate non-significant relationships ($p >$

0.05) in SEM. Numbers represent standardized path coefficients (*p < 0.05, **p < 0.01, ***p < 0.001), the magnitudes of which are proportional to the thickness of arrows (significant relationships). The bottom panel shows the direct and indirect effects on SOM priming.